Inherited CD55 Deficiency in Patients with Early Onset Protein-Losing Enteropathy and Thrombosis

SUPPLEMENTARY APPENDIX

TABLE OF CONTENTS

CONTRIBUTING AUTHORS

Ahmet Ozen[1,2,3,4,22], William A. Comrie[1,2,22], Rico Chandra Ardy[5,6,22], Cecilia Domínguez Conde[5,6], Buket Dalgic[7], Ömer Faruk Beser[8], Aaron R. Morawski[1,2], Elif Karakoc-Aydiner[3,4], Engin Tutar[9], Safa Baris[3,4], Figen Özcay[10], Nina Kathrin Serwas[5,6], Yu Zhang[2,11], Helen F. Matthews[1,2], Stefania Pittaluga[12], Les R. Folio[13], Aysel Unlusoy Aksu[14], Joshua J. McElwee[15], Ana Krolo[5,6], Ayca Kiykim[3,4], Zeren Baris[10], Meltem Gulsan[10], Ismail Ogulur[3,4], Scott B. Snapper[16], Roderick HJ Houwen[17], Helen L. Leavis[18], Deniz Ertem[9] , Renate Kain[19], Sinan Sari[7], Tülay Erkan[8], Helen C. Su[2,11], Kaan Boztug[5,6,20,21,23], Michael J. Lenardo[1,2,23]

Affiliations

[1]Molecular Development of the Immune System Section, Laboratory of Immunology, National Institute of Allergy and Infectious Diseases, National Institutes of Health, Bethesda, MD, USA

[2]NIAID Clinical Genomics Program

[3]Department of Pediatrics, Division of Allergy and Immunology, Marmara University, Istanbul, Turkey

[4]Istanbul Jeffrey Modell Diagnostic Center for Primary Immunodeficiency Diseases

[5]Ludwig Boltzmann Institute for Rare and Undiagnosed Diseases, Vienna, Austria

[6]CeMM Research Center for Molecular Medicine of the Austrian Academy of Sciences, Vienna, Austria

[7]Department of Pediatrics, Division of Pediatric Gastroenterology, Hepatology and Nutrition, Gazi University, Ankara, Turkey

[8]Department of Pediatrics, Division of Pediatric Gastroenterology, Hepatology and Nutrition, İstanbul University Cerrahpaşa Faculty of Medicine, İstanbul, Turkey.

[9]Department of Pediatrics, Division of Pediatric Gastroenterology, Hepatology and Nutrition, Marmara University, İstanbul, Turkey

[10]Department of Pediatric Gastroenterology, Hepatology and Nutrition, Faculty of Medicine, Başkent University, Ankara, Turkey.

[11]Human Immunological Diseases Section, Laboratory of Host Defenses, National Institute of Allergy and Infectious Diseases, National Institutes of Health, Bethesda, MD, USA

[12]Laboratory of Pathology, National Cancer Institute, National Institutes of Health, Bethesda, MD, USA.

[13]Radiology and Imaging Sciences, Clinical Center, National Institutes of Health, Bethesda, MD, USA.

[14]Pediatric Gastroenterology Clinic, Dr. Sami Ulus Children's Hospital, Ankara, Turkey

[15]Merck Research Laboratories, Merck & Co, Boston, MA, USA

[16]Division of Gastroenterology, Hepatology and Nutrition, Boston Children's Hospital, Harvard Medical School, Boston, Massachusetts, USA

[17]Department of Pediatric Gastroenterology, University Medical Center/Wilhelmina Children's Hospital, Utrecht, The Netherlands

[18]Dept. Rheumatology and Clinical Immunology, University Medical Center Utrecht, The Netherlands

[19]Clinical Institute of Pathology, Medical University of Vienna, Vienna, Austria

[20]Department of Pediatrics and Adolescent Medicine, Medical University of Vienna, Vienna, Austria.

[21]St. Anna Kinderspital and Children's Cancer Research Institute, Department of Pediatrics, Medical University of Vienna, Vienna, Austria

[22] and [23] These authors contributed equally to this work.

Correspondence should be addressed to Michael J. Lenardo, Chief, Molecular Development of the Immune System Section, Building 10/11D14, Laboratory of Immunology, 10 Center Dr. MSC 1892, National Institute of Allergy and Infectious Diseases, Bethesda, MD 20892-1892; e-mail - lenardo@nih.gov PHONE: (301) 496-6754 MOBILE: (301)-728-4139 or Kaan Boztug, Director, Ludwig Boltzmann Institute for Rare and Undiagnosed Diseases & CeMM Research Center for Molecular Medicine of the Austrian Academy of Sciences, Vienna & Lazarettgasse 14 AKH BT 25.3, A-1090 Vienna; e-mail: kaan.boztug@rud.lbg.ac.at; telephone number: +43 1 40160 70069; fax number: +43 1 40160 970000.

AUTHOR CONTRIBUTIONS

A.O. identified families 1, 2, 4, 6 and 7, conceived experimental plan, performed flow cytometry and complement deposition assays, and performed CD55 rescue on patient T cells. W.A.C. conceived experimental plan, performed qRT-PCR studies, performed anaphylatoxin and C3d deposition experiments, and quantified cytokine production and analyzed the effects of cytokines and ATRA on HUVEC cells. R.C.A identified CD55 mutations in families 3 and 5, performed flow cytometry, generated CD55-CRISPR knockout Jurkat cells, performed complement deposition assays on Jurkats and quantified T-cell activation and cytokine production. C.D.C. and N.K.S performed variant filtering, Sanger validation and identified the CD55 mutation in family 3. A.R.M. validated mutations in Patients 1.1 and 2.1. A.R.M. and A.O. discovered and described novel CD55 mutations in Family 6 and Family 7. A.R.M. performed immunoblotting experiments and screened EO and VEO-IBD patients for CD55 expression by flow.cytometry A.Kr. performed additional targeted sequencing of CD55 Y.Z. performed bioinformatics analyses on WES data. R.H.J.H., H.L., B.D., O.F.B., E.K.A., E.T., S.B., F.O., A.U.A., A.Ki., Z.B., M.G., D.E., M.B., S.S. and T.E. took care of and enrolled patients into the study. I.O. and A.Ki. enrolled patients, collected samples and screened potential families for CD55 deficiency by flow cytometry. S.S. and S.B.S. provided critical gastroenterologic expertise on discussion. H.F.M. coordinated clinical study protocol and sample collection. S.P. provided histopathologic evaluation of GI biopsy material. L.F. reviewed radiologic images and provided expertise. R.K performed electron microscopy and immunohistochemistry and provided expertise. J. McElwee performed/organized WES studies and analyzed data. A.O, W.A.C, R.C.A , K.B., and M.J.L. wrote the initial draft and revised version of the manuscript. M.J.L., K.B and H.C.S. supervised research and data analysis, provided ideas and advice, and edited the manuscript. All authors provided critical input and agreed to this publication.

SUPPLEMENTAL PATIENT CLINICAL HISTORIES

Patient 1.1, a 7-year-old girl born to consanguineous Turkish parents, presented with bloody diarrhea and vomiting at 4 weeks of age, and experienced repeated episodes throughout childhood (Fig. 1A and S1A). At 6 months of age, she was admitted to the hospital with persistent diarrhea, pneumonia, and facial/extremity edema, for which she received antibiotics and albumin replacement therapy. Over time she developed chronic malabsorption with micronutrient deficiencies, anemia and growth retardation (Table 1, Table S1, Fig. S2B). Endoscopic examination revealed ulcers, exudate formation (Fig. 1D) and nodularity in the colon (Table S1). The patient was treated with corticosteroids, azathioprine and mesalazine, along with supplementation of Vitamin -D and -B12, omega-3 fatty acids and enteral feeding. She received thyroxine therapy for subclinical hypothyroidism, with elevated TSH but normal T4 and free T4 levels and negative anti-thyroglobulin and anti-thyroid peroxidase antibodies. She was treated with octreotide for 12 months without any effect on albumin levels. Although the patient's gastrointestinal (GI) symptoms improved with treatment and she gained weight, long-term remission could not be achieved. The patient was placed on infliximab therapy at 6 years of age for ongoing GI symptoms, but showed little successful clinical improvement and medication was stopped after the second dose due to a systemic reaction. She also experienced a high frequency of respiratory infections beginning at 6 months of age. She was found to have pan-hypogammaglobulinemia and was treated with intravenous immunoglobulin (IVIG), leading to fewer infections. Antibody production tested with isohemagglutinin levels showed normal Anti-A and Anti-B titers. During follow up, despite IVIG treatment, trough levels of IgG remained below the desired range, and tracked with levels of serum albumin (Fig. 1B). Fecal excretion of **α-**1 antitrypsin was elevated, implying that protein-losing enteropathy (PLE) contributed to refractory hypogammaglobulinemia. Despite vitamin supplementation and dietary intervention, Patient 1.1 had persistent short stature but improved weight gain (Fig. S2B). In addition to the biallelic loss of function mutation in CD55, this patient also harbored a homozygous splice site mutation (c.2064-1G>C) in CD21, encoded by the *CR2* gene, that resulted in loss of protein expression (Fig S5A). Evaluation of B cell subsets revealed a

reduction of class-switched $IgD^{-}CD27^{+}$ memory B-cells, along with an increase in the proportion of $IgD^{-}CD27^{+}$ naïve B cells in Patient 1 compared to controls and CD21-sufficient patients (Fig S5B, S5D, and S5E).

Patient 2.1, a 22-year-old female born to consanguineous Turkish parents, presented with fever, productive cough and hemoptysis at 6 years of age and was diagnosed with pneumonia (Fig. 1A and S1B). She continued to have recurring respiratory symptoms with breathing difficulty, wheezing, chronic coughing, and multiple attacks of pneumonia leading to the development of bronchiectasis and finger clubbing. Simultaneously with the onset of respiratory symptoms, she presented with periorbital and pretibial edema, chronic GI symptoms, with abdominal pain, distention, and diarrhea, and growth retardation. Laboratory examination revealed hypoalbuminemia, decreased serum levels of Vitamin B12, folate and iron. She was commenced on thyroxin therapy for compensated hypothyroidism, with elevated TSH levels but normal thyroid hormones and negative anti-thyroid autoantibodies. At age 11, she was discovered to have hypogammaglobulinemia and was started on IVIG replacement therapy. While on IVIG, the frequency of infections decreased substantially leading to the reversal of bronchiectasis. Despite IVIG, serum immunoglobulin G levels remained low and correlated with the serum albumin levels over time, suggesting loss through the GI tract (Fig. S2A). The patient was evaluated for isohemaglutinin titers and antibody response to pneumococcal vaccine, with normal results. After several years of no follow up, she presented to the gastroenterology clinic with abdominal pain and diarrhea. Endoscopic examination revealed mucosal ulcers in the terminal ileum and mucosal nodularity throughout the colon (Table S1). Histopathology was remarkable for lymphoid aggregates in the intestinal wall. She was started on inflammatory bowel disease (IBD) medications including corticosteroids, mesalazine, azathioprine, and anti-TNF. Although she received some benefit from these medications, she developed intestinal obstruction at the age of 22 years and underwent surgery for the resection of the narrowed intestinal segment (Fig. S3D). The resection material showed dramatic lymphangiectasia (Fig. S3A) and focal inflammatory changes, including fibrinopurulent exudate, edematous villi, and neutrophil infiltration (Fig. 1D). During the short-term follow-up thus far after surgery, she has been recovering well with weight gain and normal serum protein levels. At presentation, Patient 2.1 was within the third and tenth weight and height percentiles but with her treatments

and dietary supplements, she has progressively reached the 25th and 50th percentiles for weight and height, respectively, in the most recent determinations (Fig. S2B).

Patient 3.1, a 16-year-old male born to consanguineous Turkish parents, presented with bloody diarrhea and vomiting at the age of 11 months followed by facial and extremity edema due to hypoalbuminemia at 27 months. Serial colonoscopies revealed progressive macroscopic hyperemic lesions with ulcers, cryptitis, crypt abscesses (Fig. S4B), and lymphoid cell infiltration that did not respond to IBD treatment comprising corticosteroids and azathioprine. Over time, the addition of mesalazine and supplementation therapy with calcium, vitamin B12 and folic acid led to clinical improvement. Serial measurements of serum albumin levels and immunoglobulins revealed persistent hypoproteinemia (Table S1, Fig. S2A) leading to a diagnosis of protein losing enteropathy. The patient experienced recurrent lung infections during the initial years of disease, however, his respiratory symptoms improved over time. Total lymphocyte counts were normal. He was found to be heterozygous for the *MEFV* gene (R202Q/N) and was given colchicine for suspected familial Mediterranean fever. Of note, during the GI episodes, no infectious trigger was identified and systemic inflammatory markers C-reactive protein (C-RP) levels and erythrocyte sedimentation rate (ESR) were normal.

Patient 4.1, a 3-year-old girl born to consanguineous parents, presented with puffy eyes, diarrhea and vomiting at 1 year of age. She continued to have recurrent episodes of periorbital and pretibial edema, mostly triggered by the bouts of bloody and mucous diarrhea. She was found to have persistent hypoalbuminemia, for which she received intermittent albumin infusions (Fig. S2A). Evaluation for other serum proteins revealed hypogammaglobulinemia, with low IgG, IgA and IgM levels (Table S1). At presentation, anthropometric indices revealed wasting with weight within the 3rd to 10th percentile and height within the 50th percentile for her age. The patient currently treated for vitamin B12 deficiency. Despite low immunoglobulin levels she has not yet experienced any significant or recurrent infections. Evaluation for infectious etiology during attacks of diarrhea and vomiting were negative, and she had at those times normal levels of inflammatory markers such as CRP and ESR. Evaluations for food allergy, cystic fibrosis or celiac disease were also negative.

Patient 4.2, a 17 year-old boy and brother of Patient 4.1 and 4.3, has a history of occasional and self-limiting presentations with facial and extremity edema, for which no medical intervention was required. Despite testing positive for hypogammaglobulinemia, he denied any history of infections of unusual severity or frequency. The patient has not experienced any significant GI symptoms thus far.

Patient 4.3, an 18-year-old boy and brother of patient 4.1 and 4.2, has not experienced any significant GI symptoms thus far, and has not reported any history of edema. Laboratory evaluation revealed low-normal levels of serum proteins and low vitamin B12 (Table S1).

Patient 4.4 was an affected female cousin of patients 4.1-4.3 with an unknown genotype. She presented with recurrent facial and extremity edema, chronic bloody diarrhea, chronic malnutrition, low serum protein levels, with hypoalbuminemia (albumin: 1.9 g/dl) and hypogammaglobulinemia. Histopathology of intestinal biopsies revealed the presence of dramatic lymphangiectasia in the small intestine. The patient was treated with immunosuppressive medications including steroids and azathioprine for suspected IBD. Interestingly, she had a history of thrombosis and cerebral vascular disease with a hypodense brain lesion in the lateral ventricule and received anticoagulation therapy with low molecular weight heparin. Angiographic studies demonstrated intra-abdominal and cerebral vasculopathies including, 1) narrowed superior mesenteric vein with multiple collateral veins, suggestive of chronic thrombosis, 2) decreased blood flow in internal carotid arteries, particularly in cavernous and intracranial segments and undetectable middle cerebral artery. She eventually developed an intestinal obstruction and underwent intestinal resection surgery to remove the narrow segments. At 33 years of age this patient died of thrombosis, cardiac arrhythmia, and respiratory distress syndrome developing after surgical resection to remove a severe intestinal obstruction. No genotype was obtained due to lack of patient tissue and failure to extract DNA from historical biopsy specimens.

Patient 5.1 is a 10-year-old boy and the sibling of Patient 5.2 who was born to consanguineous Turkish parents. The patient was first admitted to a hospital at the age of one year with diarrhea and vomiting. He was diagnosed with intestinal lymphangiectasia and severe hypoproteinemia, with low albumin and immunoglobulin

levels. He required frequent albumin infusions and was put on a protein-rich diet supplemented with medium-chain triglycerides (MCT). At the age of 7 years old he underwent abdominal surgery for the resection of lymphangiectatic segments, which led to a temporary abatement of his symptoms. He has had multiple recurrent thrombotic events in mesenteric veins, hepatic veins, and the inferior vena cava, as well as atrial and ventricular thrombosis. He was anticoagulated with low molecular weight heparin following cardiac surgery for atrial thrombosis. He also presented with intracranial bleeding and underwent neurosurgical operations. Currently, the patient is prescribed octreotide intermittently. He does not have increased respiratory infections despite low immunoglobulin levels. He has had no evidence of gastrointestinal infection, and sweat chloride test, celiac markers, and lipid profiling were normal. Colonic biopsy revealed edema and eosinophilic infiltrates, from which a diagnosis of eosinophilic colitis was made. The patient was homozygous for the A1298, allele of the methylenetetrahydrofolate reductase (*MTHFR*) gene, although homocysteine levels were normal, suggesting no increased risk of thrombosis attributable to hyperhomocysteinemia. The patient was tested twice for paroxysmal nocturnal hemoglobinuria (PNH). Though these results showed low CD55 expression on $CD16^{+}$ cell populations, CD59 expression was normal. Additionally, evaluation by the Fluorescein-labeled proaerolysin (**FLAER**) flow cytometry assay, which detects the GPI anchor that is absent on cells affected by PNH, and staining for other GPI linked proteins revealed no defect on patient peripheral blood mononuclear cells (PBMC). Currently, the patient is in poor condition and requires frequent hospital admissions. In addition to the homozygous CD55 mutation, we identified a homozygous missense variant in CD27 (c.709C>A, p.P237T) which was predicted to be deleterious (CADD score 29.4, SIFT 0.02 deleterious, Polyphen2 (0.96) probably damaging). This mutation did not reduce CD27 surface expression and did not alter naïve or class-switched B cells subset (Fig. S5C, S5D, and S5E). Patient 5.1, has a low positive measurement for Epstein-Barr Virus (420 copies/mL) presently without clinical disease but under regular clinical follow up since CD27 deficiency is associated with an increased risk of EBV-driven lymphoproliferative disease. The patient is also positive for anti-EBV IgG indicating that an appropriate class switching response to EBV was achieved.

Patient 5.2, is the 12-year-old affected sister of Patient 5.1. She presented with frequent abdominal pain, recurrent self-limiting intestinal obstruction, and hypogammaglobulinemia and hypoalbuminemia that required frequent albumin transfusions. Due to episodes of intestinal obstruction, she underwent resection of edematous small bowel segments, which were found to contain lymphangiectatic segments, which resulted in temporary clinical remission. Post-surgery follow up revealed that the patient still experiences recurrent abdominal pain and intestinal obstructions. This patient did not present with any thrombotic events, infectious history, or bloody diarrhea. Testing for EBV viral load showed a low positive measurement (100 copies/mL)

Patient 5.3, an affected sister of patients 5.1 and 5.2 of unknown genotype, was admitted at 15 months old with complains of eyelid and extremity edema and diarrhea. She had hypoalbuminemia, hypogammaglobulinemia, thrombocytosis, and anemia. Endoscopy and histopathological examination of the duodenal biopsies revealed intestinal lymphangiectasis. She had severe malnutrition, with reduced levels of calcium, magnesium, phosphorus, and various vitamins. She was treated with intravenous calcium, albumin, vitamin, mineral supplements, medium chain triglyceride supplements, and octreotide. These treatments led to temporary clinical improvement. Small bowel resection was performed three times over a period of 2 years with only transient clinical improvement. Parenteral nutrition efforts were interrupted by *Candida* and *S. aureus* infections along with sepsis. She developed a thrombus in the vena cava superior leading to vena cava superior syndrome and anti-thrombotic treatment with low molecular weight heparin and tissue plasminogen activator was initiated. The patient developed ascites, pleural effusion, and pulmonary infection and died when she was 4.5 years old.

Patient 6.1, was a 15-year-old boy born to consanguineous Turkish parents, presented with facial and extremity edema at 1.5 years of age and was found to have hypoalbuminemia. He had frequent hospital admissions due to vomiting, diarrhea and abdominal pain. Endoscopic examination revealed intestinal lymphangiectasia and he was put on corticosteroids. Evaluations for common causes of secondary lymphangiectasia including heart diseases and abdominal mass lesions were negative. Because of persisting

symptoms he was started on octreotide treatment and prescribed a diet low in fat and high in protein along with MCT supplements. Along with chronic gastrointestinal symptoms he developed deficiencies in the major micronutrients and vitamins such as iron, calcium, magnesium and vitamin D, leading to growth retardation. Frequent exacerbations of facial and extremity edema and abdominal symptoms associated with severe intestinal wall edema required repeated albumin transfusions. Consistent with low albumin levels, serum immunoglobulins were decreased (Table 1). Apart from chronic gastrointestinal symptoms, he experienced frequent respiratory symptoms with chronic cough and finger clubbing. Computer tomography of the chest revealed fibrotic changes in the posterobasal lung segments. When he was 14 years of age, he suffered severe thrombotic events, with a thrombus originating from a stalk 2 cm distal to the inferior vena cava (IVC) extending into the right atrium that was impairing venous blood flow. He also had thrombi in the pulmonary arteries. He underwent thoracic surgery for thrombectomy and was anticoagulated with low molecular weight heparin and low dose aspirin. Despite prophylactic anticoagulation treatment, during follow up he experienced recurrence of thrombosis with reformation of the clot in the right atrium. Screening for common congenital hypercoagulable states such as Factor V Leiden or prothrombin G20210A mutations that lead to overactivity of coagulation factors, or arising from a deficiency of the natural anticoagulants Protein C, S and anti-thrombin III, was negative. The patient demonstrated significant growth retardation, worsening after age 14 when the patient developed severe thrombosis (Fig. S2B). He was found to be heterozygous for the thermolabile variant of *MTHFR*, C677T. However; the *MTHFR* A1298C mutation was not observed, and the patient had normal plasma homocysteine, suggesting no increased risk of thrombosis attributable to hyperhomocysteinemia. The patient was also tested for anti-cardiolipin and anti-phospholipid antibodies and for paroxysmal nocturnal hemoglobinuria, through the FLAER flow cytometry assay, with negative results. The patient continued to require frequent hospital admissions and ultimately passed away of a pulmonary embolism at 15 years of age.

Patient 7.1, a 4-year-old girl born to consanguineous Syrian parents, presented with facial and extremity edema at 1 year of age, with continued relapses thereafter. She has experienced recurrent gastrointestinal symptoms, with chronic diarrhea and was found to have hypoalbuminemia. She was diagnosed with suspected

intestinal lymphangiectasia and given octreotide. She has growth retardation, with height for age below the 3rd percentile. Due to micronutrient deficiencies she received supplementation therapy with vitamin D, vitamin B12 and multivitamins, as well as blood transfusion for anemia. She was prescribed a diet low in fat and high in proteins, MCT supplements, and further supplementation by enteral feeding and albumin transfusion as required. Measurement of serum immunoglobulins revealed low IgG, IgA and IgM (Table 1). Patient 7.1 has a current height for age value below 3rd percentile (Fig. S2B). Immunologic evaluation revealed normal isohemagglutinin titers and lymphocyte subsets were normal. She has experienced recurrent lower respiratory infections and received parenteral antibiotics and was put on prophylactic antibiotics with co-trimoxazole.

Patient 8.1, a 15-year-old girl born to consanguineous parents of Moroccan origin presented with diarrhea and abdominal pain (present only when serum albumin is low) at 5 years of age. Clinical evaluation revealed ascites and low serum proteins (albumin and gammaglobulins) and micronutrient deficiencies, with low iron, ferritin and Vitamin D. The patient was diagnosed with PLE and intestinal malabsorption syndrome and has been treated with monthly albumin transfusion therapy to replace ongoing GI protein losses as well as vitamin D, iron, and vitamin K supplementation. Serial endoscopic examinations of the lower GI tract revealed inflammatory cell infiltrates in the colonic mucosa, mainly consisting of lymphocytes and plasma cells and a single endoscopy taken when she presented with hematochezia showed a solitary polyp in the ascending colon, with histologic features characteristic of a juvenile polyp. Overall, her intestinal pathology is characterized by an atypical and indeterminate intestinal inflammation with no histopathology of classical IBD. Upper GI examinations have been largely normal so far. Of particular interest the patient developed liver cirrhosis and hepatosplenomegaly at a young age and was found to have Budd-Chiari syndrome underlying her liver disease. She was treated with transjugular intrahepatic portosystemic shunt (TIPS) to relieve portal hypertension at 8 years of age and was commenced on low dose acetyl salicylic acid to prevent TIPS occlusion. Further, a banding procedure was performed [at 8 years] at that time to treat esophageal varices. Additionally, the patient has joint disease characterized by hypertrophic osteoarthropathy (finger clubbing) with periostitis in small joints and knees along with arthritis for which she receives methotrexate, meloxicam, and bi-

monthly 40 mg subcutaneous Humira® therapy since 12 years of age to treat the arthritis. She was also diagnosed with hypothyroidism at 14 years of age, and has been receiving thyroxine therapy. While the patient shows normal growth, she has had delayed onset of puberty for which estradiol treatment was prescribed.

SUPPLEMENTAL MATERIALS AND METHODS

Human Subjects

All human subjects (or their legal guardians) provided written informed consent in accordance with Helsinki principles for enrollment in research protocols that were approved by the Institutional Review Boards of the National Institute of Allergy and Infectious Diseases, National Institutes of Health (NIH) or the CeMM Research Center for Molecular Medicine of the Austrian Academy of Sciences. Patient and healthy control blood was obtained at the respective Turkish institutions overseeing patient care under approved protocols, and shipped to either the NIH or the CeMM Research Center for Molecular Medicine of the Austrian Academy of Sciences. Additional healthy control blood was obtained at the NIH Clinical Center under approved protocols. As described previously, mutations will be automatically archived by Online Mendelian inheritance in Man (OMIM) at time of publication, and whole-exome data will be submitted in dbGaP. We will also create a webpage through National Center for Biotechnology Information (NCBI) to accumulate patient mutation data in the format of the Leiden Online Variant Database (LOVD) as patients are identified.[1]

Genetic Analysis Methods

Genomic DNA (gDNA) was obtained from probands and family members by isolation and purification from peripheral blood mononuclear cells (PBMCs) using Qiagen's DNeasy Blood and Tissue Kit. DNA was then submitted for Whole Exome Sequencing (WES) or targeting sequencing of the CD55 gene. For whole exome sequencing the Human All Exon 50 Mb kit (Agilent Technologies) coupled with massively parallel sequencing by Illumina HiSeq Sequencing System was performed using the collected DNA. For individual samples, WES produced 50–100x sequence coverage for targeted regions. WES was performed on patients 1.1, 2.1 along with 3.1 and 5.1 in which WES was combined with homozygosity mapping. As described previously, all sequenced DNA reads were mapped to the hg19 human genome reference by Burrows-Wheeler Aligner with default parameters. Single nucleotide variant and indel calling were performed using the Genome Analysis

Toolkit (the Broad Institute). All SNVs/indels were annotated by SeattleSeq Annotation together with an in-house custom analysis pipeline that was used to filter and prioritize for autosomal recessive or de novo putative disease-causing variants. Based on the clinical pedigree for Patients 1.1 and 2.1, the mutations were identified by targeted gene screening of the WES data based on the clinical phenotype defined in the cohort.[2]

For targeted sequencing, CD55/DAF (CD55: NCBI NG_007465.1) exons 1 through 10 were PCR-amplified, purified, or gel-extracted using Qiagen's miniElute PCR Purification Kit or Qiagen's gel extraction kit, respectively. Samples were submitted to the National Institute of Allergy and Infectious Disease Research Technologies Branch Core Sequencing facility for Sanger sequencing. DNA sequences were analyzed using Sequencher V.5.3. The following primers were used for Sanger sequencing.

Exon #	Forward Primer Sequence	Reverse Primer sequence
Exon 1	CTACTCCACCCGTCTTGTTTGT	TTTGGGGGTTAAGGATACAGTC
Exon 2	CAGGTGTGGCATTTCAAGG	ACCCTGGGGTTTAGTAACGC
Exon 3	AAGTACTAAATATGCGCAAAGCAG	ATGGTCCTATCAAGAAACATCC
Exon 4	GTTACCTTCTTTGTGTGTATGCC	GCTGTGAATACCAGTCATGAAAC
Exon 5	AACCTGGAGAATTTGAGGAAAG	TGTGCTAATATTCTTAAGGGGC
Exon 6	GCATTTATAAGCATCTCTTGTTGG	TCATTGAATGTCTGCAACCC
Exon 7	CTAGGTGTTTGTGGGGAGAGAG	TCTGGTGGGTTTCTGAAGAGTT
Exon 8	TTTACGCAGAGTCCTTCAGC	CCATTTAATCCTGCAATCTTGG
Exon 9	TGGAAATTTGAGTTGCTTTCG	TCTCCCAGGAATATGGATTG
Exon 10	GCACCCCAAATTAACTGATTC	ATGTGATTCCAGGACTGCC

Primary cells and Cell lines

Patient or control blood was subjected to a Ficoll density gradient centrifugation, after which peripheral blood mononuclear cells (PBMCs) were collected from the interface. Naïve or total $CD4^+$ T cells were then isolated by negative selection using the Naive $CD4^+$ T Cell Isolation Kit II or the human $CD4^+$ T cell isolation kit, respectively (Miltenyi). Jurkat E6, and HEK 293T cells were purchased from the American Type Culture Collection (ATCC). Pooled Human Umbilical Vein Endothelial Cells (HUVECs) were from Lonza.

Media

Human T cells and Jurkat T cells were either grown in RPMI 1640 (Gibco / Thermo Fisher) supplemented with 10% heat inactivated FBS (Gibco / Thermo Fisher), 1% Penicillin / Streptomycin, 1% L-Glutamine and 100 units/mL IL-2 (complete RPMI) or X-Vivo 15 (Lonza) supplemented with 1% Penicillin/Streptomycin, 1% L-Glutamine and 100units/mL IL-2 (complete X-vivo 15). HEK293T cells were grown in DMEM medium (Gibco / Thermo Fisher) supplemented with 10% heat-shocked FBS (Gibco / Thermo Fisher), 1% Penicillin/Streptomycin, and 1% L-Glutamine. HUVECS were cultured in Endothelial Cell Basal Medium (Lonza) supplemented with the contents of EGM SingleQuot Kit Suppl. & Growth Factors kit (Lonza).

Human Serum and Plasma Preparation

Human serum was collected from the NIH donor program from healthy normal controls and stored at -20°C until use. On the day of experiments, serum from at least three donors was thawed and pooled. If the serum was to be heat inactivated, 1mL aliquots were heated to 37°C with shaking for 30 minutes. Serum was then spun at 15,000xG for 10 minutes at 4°C to remove large aggregates. Serum was then immediately used in experiments. As the coagulation reaction can produce large amounts of anaphylatoxins, we found we had to use human plasma to measure anaphylatoxin production. Blood was drawn into EDTA tubes and overlayed on a Ficoll density gradient and spun at 2000rpm for 20 minutes. The plasma component was then collected and stored at -20°C until use. On the day of the experiments, plasma samples from at least 2 donors were thawed, pooled, and spun at 15,000xG for 10 minutes at 4°C to remove large aggregates. Plasma samples were then washed twice with 5mLs of PBS + 10uM EDTA over a 30kD cutoff Amicon centrifugal filter device in order to remove preformed anaphylatoxins. Proteins were then resuspended in PBS + 10uM EDTA to original plasma concentrations. Immediately prior to use, Ca^{2+} and Mg^{2+} were added at a final concentration of 10uM each in order to reconstitute the complement activation pathways that are dependent on these cations.

Antibodies and Inhibitors

Anti-CD25 FITC, Anti-CD69 APC, Anti-CD4 PE, Anti-CD55 FITC or PE, anti-CD59 FITC, anti-CD46 APC, anti-

CD141/Thrombomodulin APC, anti-CD142/Thrombin PE, and anti-CD28 (clone CD28.2) were purchased from Biolegend or eBisociences. Anti-C3b antibody was from abcam. The anti-C3d antibody used in complement deposition experiments was from Hycult biotech. LIVE/DEAD™ Fixable Near-IR Dead Cell Stain Kit used for cell viability assay was from ThermoFisher Scientific and the APC-labeled Annexin-V was from Biolegend. The anti-CD3 antibody HIT3α used in T cell re-stimulation experiments was purchased from Biolegend. The anti-CD55 antibody (clone BRIC 216) used to costimulate T cells was from EMD Millipore or IBGRL. Anti-CD55 used for western blotting was from Sigma-Aldrich. For immunohistochemistry and indirect immunofluorscence, the following antibodies were used: CD55 catalog number HPA024386 is from Atlas Antibodies, C3c (catalog number A0062) is from Biozol, C4d (catalog number BI-RC4D) is from Biomedica, C5b-9 (catalog number M0777) and CD31 (catalog number M823) are from Agilent. Human CD97-Fc recombinant protein used for T cell costimulation was from Creative Biomart. The C3aR inhibitor, SB 290157, was from Calbiochem. The C5aR1 inhibitor, NDT 9513727, was from TOCRIS bioscience. TT30, m5G1.1 and relevant isotype control antibodies were a gift from Alexion pharmaceuticals.

Electron Microscopy

Duodenal biopsy was fixed in 4% formaldehyde/1% glutaraldehyde in 0.1M phosphate buffered fixing solution prior to processing to Epoxy resin. Images were taken on a *Jeol* JEM-1010.

Immunohistochemistry (IHC) and indirect immunofluorescence (IIF)

IHC was performed according to previously published protocols using antibodies mentioned above.[3] Images were taken on a Nikon Microphot SA equipped with a ProgRes C5 camera (Jenaoptik) using the ProgRes Image Capture Pro software. Indirect double IIF was performed using established staining protocols (see Hubert et. al, 2016) and sections viewed and pictures taken using a confocal laser scanning microscope (LSM 5 exciter, Carl Zeiss) using ZEN 2009 software.[4]

Flow Cytometry

Adherent cells were treated with 0.05% trypsin EDTA to lift them from the surface followed by addition of 5% FBS to inactivate the trypsin. Suspension cells were collected from culture following mixture of the culture by repeat pipetting. Cells were washed and resuspended in FACS buffer (1% FBS, 0.05% sodium azide, and 5mM EDTA in PBS) at $2x10^6$ cells/ml. Staining or isotype antibodies were added at 1:200 final dilutions and incubated with cells at 4°C for 30minutes to 1hr. Cells were then washed 3X and resuspended in FACS buffer with 1% PFA and analyzed by flow cytometry. In cases where surface vs. total cellular expression of a molecule was determined, cells were fixed in 4% PFA in PBS for 20 minutes, washed and then either left alone or permeablized with 0.1% Triton X-100 in PBS. Cells were then extensively washed and stained as previously mentioned. Flow files were analyzed on FlowJo version 9.9 or above and unless otherwise indicated all flow plots are presented on a log10 axis and histograms are presented as % of max expression for the Y-axis.

Complement Activation

T cells (Patient $CD4^+$ T cell blasts or Jurkat T cells) were collected and washed 3X in basal RPMI. Cells were then resuspended in basal medium and rested for 2-3 hours at 37°C to allow any deposited complement components to be cleared from the cell surface. Rested cells were then collected and resuspended in basal RPMI or basal RPMI that had been adjusted to pH 6.5 (acidified media) to a final concentration of $1x10^6$ cells/mL. Non-heat inactivated pooled normal human serum was then added to cell suspension for the indicated amount of time. Human serum that had been heat inactivated at 56°C for 30 minutes was used as a negative control for complement activation. At the indicated times cells were transitioned to 4°C, and kept chilled for the remainder of the experiment. In some experiments cells were pre-coated for 30 minutes at room temperature with aCD28.2 as an activator of the classical complement pathway. Cells were then washed 3X in PBS and resuspended in basal media with 10% human plasma, prepared as previously described. Cells were then incubated for 1hr at 37 °C. For measurements of C5a production, cells were collected as previously described and $1x10^6$ cells were resuspended in 100uL of basal X-vivo15 media with 10% human plasma and the indicated antibodies (Isotype control or m5G1.1) at a final concentration of 10ug/mL. Cells were then incubated for 2hr at 37 °C before 20uL of supernatants (SN) were collected and immediately placed into 180uL

of 10uM EDTA in PBS to prevent further complement activation. Samples were then immediately analyzed or frozen at -80 ^{o}C For complement deposition, cells were stained with a 1:300 dilution of anti-C3d antibody for 30 minutes, washed 3X and then stained with an anti-rat antibody conjugated with Alexa Fluor 488 at a 1:500 dilution for 30 minutes. Cells were washed 3X and resuspended in FACS buffer (PBS, 1%FBS) and analyzed for C3d deposition by flow cytometry. For determination of anaphylatoxin production, the saved SN were diluted 1:10 in PBS + 10uM EDTA, for a final dilution of 1:100 of the original 10% plasma used in the experiments, and analyzed using the Human Anaphylatoxin Cytometric Bead Array from BD.

Preparation of T cell stimulatory surfaces

Tissue culture treated 48, or 96 well plates were incubated with the indicated concentration of anti-CD3 in PBS for 2hrs at 37^{o}C. Plates were then washed 3X in PBS and incubated with either anti-CD28, anti-CD55, or CD97-Fc for 2hrs at 37^{o}C. Plates were again washed 3X with PBS before using in T cell stimulations.

T cell stimulation and cytokine secretion

To measure T cell activation isolated CD4 T cells were either left alone or stained with 1 μM CFSE for 5 minutes at room temperature, protected from light. Labelled cells were washed 3X in complete RPMI prior to use and resupended at 1x10^{6} cells/mL in complete RPMI. Cells were then added to stimulatory surfaces, pre-coated with the indicated concentrations of activating antibodies / proteins. To measure CD25 and CD69 upregulation, non-CFSE labeled T cells were collected after 24 hours and analyzed by flow cytometry for CD25 and CD69 expression, as detailed above. To assess T cell proliferation CFSE-labeled T cell cultures were collected after 96 hours of stimulation and analyzed by flow cytometry for CFSE dilution.

For cytokine secretion upon primary stimulation, Naïve CD4^{+} T cells were isolated via negative selection using the Naive CD4^{+} T Cell Isolation Kit II, human isolation kit (Miltenyi). Naïve T cells were then resuspended in

complete X-Vivo15 medium. CD3/28 T cell activator Dynabeads (Invitrogen) were then added to cells (1bead/ 2 cells) and cells and Dynabeads were centrifuged at 300xG for 5 minutes to complex beads and T cells. Cells were resupended and added to 48 well plates at a final concentration of $5x10^4$ / mL in complete X-vivo15 media. Cell culture supernatants were collected every 24 hours starting at 96 hours post-activation for the indicated time course. Cell cultures were stored at -80^{o}C until analyzed. To analyze cytokine secretion upon restimulation, cells were collected from day 12 to 14 of culture in complete X-Vivo15 media, washed and resuspended in basal media at 37^{o}C for 3 hours to rest. Cells were then collected and resuspended in complete X-Vivo15 media and stimulated for 48 hours at 37^{o}C with 1 µg/mL plate-bound anti-CD3. Cell supernatants were then collected and stored at -80 ^{o}C until analyzed. When indicated, % of max control indicates that all values from an individual experiment were normalized with the maximum value for the average of the healthy donor controls across the entire timecourse set equal to 100%. Once values were normalized, multiple experiments/ repeated measurements were averaged to obtain error bars and statistics.

Lentiviral Construction and Transfection protocol

Lentiviral packaging constructs psPAX2 and PDM2.G were kind gifts of Dr. Nir Hacohen, Broad Institute. shRNA constructs against CD55 or empty vector were purchased from Sigma-Aldrich. To generate lentiviral particles, $1.2x10^6$ HEK293T cells were seeded in each well of a six well plate the day prior to transfection. Cells were then cotransfected using lipofectamine 2000 (Invitrogen) with 900 ng of psPAX2 and 100 ng of pDM2.G, together with 1 μg of the vector of interest (shRNA or lentiCRISPRv2). Alternatively, lentivirus was produced by the conventional calcium chloride transfection method. Supernatants were harvested 24 and 48 hours after transfection and frozen at -80^{o}C. HT29 cells were transduced by spin infection with lentivirus. Lentivirus and 8 µg/ml Polybrene (Sigma-Aldrich) were added to the wells of a 24-well culture plate and centrifuged at 2000 rpm and 37°C for 2 hours. Lentivirus-containing media was then replaced with 293T media, and the cultures were maintained as described above. On day 5 of culture, puromycin (Sigma-Aldrich) was added to a final concentration of 2 μg/ml to

select for virally transduced cells. Selected cells were maintained in 2 μg/mL puromycin following initial selection.

CRISPR materials/methods

The lentiCRISPR v2 was a gift from Feng Zhang (Addgene plasmid # 52961). CRISPR guide RNAs targeting *CD55* were designed using an online tool (crispr.mit.edu) as previously described and cloned into the lentiCRISPRv2 vector.[5,6] CRISPR lentivirus was produced according to the above protocol. Transductions were performed as above, with minor changes. For Jurkats, selection with 1ug/mL puromycin was performed for 3 days.

HUVEC experiments

HUVEC grown to 80% confluence, and before passage 8, were trypsinized and replated in 24 well tissue culture plates at 200,000 cells/ well in HUVEC media. 24 hours later the indicated concentrations of TNF, IL10, IFNγ, or all trans retinoic acid (ATRA) were added. 24 hours later in the cast of TNF or IL10 treatment or 48 hours later in the case of ATRA cells were trypsinized and stained for the indicated surface markers following the described flow cytometry staining protocol. Cells were then immediately analyzed.

Quantitative RT-PCR

Total RNA was isolated with the RNeasy kit (Qiagen). cDNA was synthesized from 1ug of total RNA using the SuperScript III First-Strand Synthesis System (Thermo Fisher Scientific). cDNA was brought to a total volume of 100μL in double distilled (DD)H_2O and either immediately used or stored at -80°C for future use. Quantitative RT-PCR for CD55 and GAPDH was performed using the Power Syber green (Thermo Fisher) method on a 7900HT machine (ABI) using 2.5uL of cDNA reaction product. Results were analyzed by the $\Delta\Delta C_t$ method and normalized to the first healthy normal donor values.

Western Blotting

CD4+ T cells were washed in PBS and lysed on in 1% Triton X-100, 50 mM Tris-Cl, pH 8, 150 mM NaCl, 2 mM EDTA, complete protease inhibitor cocktail (Roche), and phosphatase inhibitor cocktails (Sigma-Aldrich) on ice for 20 minutes. The lysates were then clarified by centrifugation at 15,000 g at 4°C for 10 min. Protein concentration was determined by BCA assay (Thermo Fisher Scientific). Lysates were then diluted with 2X SDS sample buffer (Quality Biologicals) supplemented with 1X sample reducing agent (Thermo Fisher Scientific). Approximately 5 µgs of total protein was separated by SDS-PAGE on 4-20% precast gels (Invitrogen) and transferred to a nitrocellulose membrane (Bio-Rad Laboratories). Membranes were blocked with 5% nonfat dry milk in Tris-buffered saline (TBS) with 0.01% Tween-20 (TBST) for 1 hour at room temperature before incubating with primary antibody overnight at 4°C. After 3x 5 minutes washes with TBST at room temperature with rocking, HRP-conjugated secondary antibody was added for one hour at room temperature. After 3x 5 minute washes, HRP substrate (Luminata Forte; Millipore) was added to the membranes, which were then developed and analyzed using the FujiFilm LAS4000 Luminescent Image Analyzer and accompanying software, LAS4000IR v2.1

Statistical analysis

Unless otherwise indicated flow plots are representative of at least three independent experiments and graphs and standard deviations are generated by averaging at least three independent experiments. Statistics were computed using the analysis options in Prism (Graphpad). Either the Mann-Whitney U test or a two-tailed unpaired T test with Welch's correction was used to compare sample means. * = $p<.05$, ** = $p<.01$, *** = $p<.001$, **** = $p<.0001$.

SUPPLEMENTAL FIGURES

Table S1. Extended Demographic and clinical characteristics of patients with CD55 deficiency.

Symptoms at first clinical presentation are indicated by red text. Numbers in boldface indicate values below the normal range. NA: Information not available. N/A: Not applicable (P4.2 and P4.3 were not evaluated by endoscopy). F: female. M: male. PLE: protein-losing enteropathy. CT: computerized tomography. IVC: Inferior vena cava. Vit.: vitamin; IVIG: intravenous immunoglobulin. MTHFR: methylenetetrahydrofolate reductase.

Table S1. Extended Demographic and clinical characteristics of patients with CD55 deficiency.

Patient ID.	**P 1.1**	**P 2.1**	**P 3.1**	**P 4.1**	**P 4.2**	**P 4.3**	**P 4.4***	**P 5.1**	**P 5.2**	**P 5.3***	**P 6.1**	**P 7.1**	**P 8.1**
Demographics													
Current age (yrs) and gender	8, F	23, F	17, M	3, F	17, M	18, M	Deceased (33), F	11, M	13, F	Deceased (4.5), F	Deceased (15), M	4, F	15, F
Age of clinical onset	6 months	6 years	11 months	1 year	2 years	None	NA	1 year	10 years	15 months	18 months	1 year	5 years
Disease manifestations													
Facial and extremity edema	Yes	Yes	Yes	Yes	Yes	None	Yes	Yes	Yes	Yes	Yes	Yes	None
GI symptoms	Vomiting, bloody and mucous diarrhea	Abdominal pain, diarrhea, vomiting	Vomiting, bloody diarrhea	Vomiting, bloody and mucous diarrhea	None	None	Chronic Bloody Diarrhea	Diarrhea and vomiting	Abdominal pain, recurrent intestinal obstruction	Diarrhea	Vomiting, abdominal pain, mucous diarrhea	Mucous diarrhea	Abdominal pain, diarrhea
Clinical outcome	PLE persists, with growth retardation, requires frequent albumin infusion	Underwent surgery for intestinal obstruction. In the short term follow-up post-surgery normal albumin levels	PLE persists, requires intermittent albumin infusion	PLE persists, retarded growth, requires frequent albumin infusion	Asymptomatic with subclinical hypoproteinemia	Asymptomatic, mild hypogammaglobulinemia	Persistent PLE with hypoalbuminemia and hypogammaglobulinemia. Intestinal resection to remove obstruction. Died at 33YOA of thrombosis, cardiac arrhythmia, and respiratory distress syndrome following surgical intestinal resection.	Resection of localized lymphangiectasis led to an intermittent recovery of PLE, which recurred. Currently suffers a debilitating disease with frequent hospital admissions and albumin transfusion	Hypoalbuminemia alleviated after surgical resection of lymphangiectatic segments	Persistent hypoalbuminemia and hypogammaglobulinemia, severe malnutrition with vitamin and micronutrient deficiencies, multiple small bowel resection. Patient passed away due to multiple complications.	Severe PLE, required frequent albumin infusion, unstable GI disease and thrombosis. Patient passed away due to thrombotic embolism.	PLE persists, impaired growth and lung infections, requires frequent albumin infusion	PLE persists requiring monthly albumin infusion
Serum Proteins													
Albumin (g/dl)	**2.3** (3.5-5.4)	**1.9** (3.5-5.4)	**1.0** (3.5-5.4)	**1.4** (3.5-5.4)	**3.2** (3.5-5.4)	4.5 (3.5-5.4)	**1.3** (3.5-5.4)	**2.2** (3.8-5.4)	**2.0** (3.8-5.4)	**2.0** (3.5-5.4)	**0.8** (3.5-5.4)	**1.6** (3.5-5.4)	**2.2** (3.5-5.4)
IgG (mg/dl)	**150** (745-1804)	**186** (876-2197)	**143** (549-1584)	**143** (604-1941)	**321** (913-1894)	**699** (913-1894)	**647** (751-1560)	**184** (886-2530)	**493** (976 – 2120)	NA	**157** (604-1941)	**240** (648-2010)	**372** (520-1560)
IgM (mg/dl)	**33** (78-261)	**49** (75-440)	39.2 (23-259)	**44.9** (71-235)	**49** (88-322)	**78** (88-322)	**43** (46-304)	75.5 (67.7-527)	96.8 (78.8-370)	NA	**24** (71-235)	**39** (52-297)	46 (28-240)
IgA (mg/dl)	**28** (57-282)	**53** (100-447)	**21.3 (**61-348**)**	**10.5** (26-296)	**43** (135-378)	146 (135-378)	NA	151 (27-198)	**11** (97.8-456)	NA	**25** (26-296)	**35** (44-244)	110 (70-360)
GI Malabsorption features													
Growth retardation	**Yes**	**Yes**	**Yes**	**Yes**	No	No	NA	**Yes**	**Yes**	**Yes**	**Yes**	**Yes**	No
Anemia	**Yes**	**Yes**	**Yes**	**Yes**	No	No	NA	**Yes**	**Yes**	**Yes**	**Yes**	**Yes**	**Yes**
Micronutrient def.	Low vit.-D and -B12	Low iron, ferritin, folate, vit-B12	Low vit-B12, calcium	Low vit-B12	Low ferritin	Low vit-B12	NA	Low iron, vit-B12, calcium, and other nutritional deficiencies	Low iron, vit-B12, and other nutritional deficiencies	Low calcium, magnesium, phosphorus, and various vitamins	Low calcium, iron, ferritin, folate, magnesium, vit-D	Low iron, ferritin, vit -D and -B12	Low iron, ferritin, vit-D
Demonstrated lymphangiectasia	No	Yes	No	No	N/A	N/A	Yes	Yes	Yes	Yes	Yes	Yes	No
GI exam; endoscopy and imaging	Mucosal ulcers in terminal ileum, lymphoid aggregates; intestinal wall thickening on abdominal CT	Mucosal ulcers in terminal ileum, lymphoid aggregates. Dilatation of intestinal segments on CT	Mucosal ulcers, cryptitis and crypt abscesses, lymphoid infiltration	Lymphoid aggregates in the colonic biopsies	N/A	N/A	Histopathology of intestinal biopsies revealed the presence of dramatic lymphangiectasia in the small intestine.	Ulceration, epithelial erosion, chronic inflammation, and dilated lymphatics in the small intestine mainly jejunum	Dilated lymphatic vessels in submucosal and subserosal small bowel	Endoscopy and histopathological examination of the duodenal biopsies revealed intestinal lymphangiectasis	Dilated lymphatic vessels in duodenum. Slender villi and a prominent lymphoid aggregate. Bowel wall thickening by radiological imaging	Non-specific duodenitis, intestinal lymphangiectasia in duodenum	Low level lymphocyte and plasma cell infiltration of colonic mucosa, juvenile polyp, upper endoscopy normal
Respiratory manifestations	Recurrent infections	Recurrent pneumonia, chronic coughing, and hemoptysis, bronchiectasis resolved with IVIG Rx	Recurrent lung infections	None	None	None	NA	None	None	Yes, Pulmonary Infections	Recurrent infections, fibrotic changes in lung CT	Recurrent pneumonia	None
Vascular features	None	None	None	None	None	None	Yes, Thrombosis and Cerebral Vascular Disease. Intra-abdominal and cerebral vasculopathies	Multiple thrombi in mesenteric and hepatic veins and right atrium	None	Yes, thrombus in the vena cava superior	Multiple thrombi in IVC, heart, and pulmonary arteries	None	Budd-Chiari syndrome
Other systemic features	Autoantibody negative hypothyroidism, osteopenia, finger clubbing, increased fecal α-1 antitrypsin level	Autoantibody negative hypothyroidism, finger clubbing	Arthralgia	Thrombocytosis, finger clubbing, transient proteinuria at the onset of symptoms	None	None		Finger clubbing, thrombocytosis, homozygous for MTHFR A1298C polymorphism, with normal homocysteine levels	Thrombocytosis	Thrombocytosis	Low complement C3, clubbing, transient proteinuria at the onset of symptoms. Hepatosplenomegaly, left renal agenesis, Cervical 5-6 hemivertebrae, scrotal hernia, developmental delay	None	Hepatospenomegaly and cirrhosis, esophageal varices, hypothyroidism, extreme finger clubbing, arthritis, delayed puberty
Medications													
Supportive Rx	Vit -D and –B12 replacement, intermittent infusions of albumin, enteral feeding, omega-3 fatty acids	Vit-B12 replacement, intermittent infusions of albumin, enteral feeding, folate, iron. Erythrocyte transfusion for once	Vit-B12 replacement, folate, calcium	Vit-B12 replacement, intermittent infusions of albumin	No treatment	No treatment	NA	Albumin infusion once every two weeks. Medium chain triglyceride and vitamin supplemented diet	Albumin infusion once every two weeks	Intravenous calcium, albumin, vitamin, mineral supplements, medium chain triglyceride supplements, and octreotide	Albumin infusion, multivitamin, calcium supplementation, vit-D, iron, magnesium, medium chain fatty acids, zinc, enteral feeding	Albumin infusion, vit -D and –B12 replacement, erythrocyte transfusion for once	Albumin infusion, diuretics (spironolacton and furosemide), Vitamin D, K, Iron supplementation
IBD/ GI Rx	Corticosteroids, mesalazine, azathioprine, anti-TNF (single dose)	Corticoteroids, mesalazine, azathioprine, anti-TNF	Corticoteroids, mesalazine, azathioprine.	None	None	None	Steroids and azathioprine	None	None	None	None	None	None
Other Rx	Octreotide, IVIG+ cotrimoxazole, thyroxin	IVIG+ cotrimoxazole, thyroxin	Colchicine for suspected FMF	None	None	None	Anticoagulation therapy with low molecular weight heparin	Octreotide, low molecular weight heparin	None	Anti-thrombotic treatment with low molecular weight heparin and tissue plasminogen activator	Corticoteroids for lymphangiectasia, octreotide, low molecular weight heparin and aspirin, amitriptyline for headache	Octreotide, cotrimoxazole, IV antibiotics for pneumonia	Thyrax, estradiol, low dose acetyl salicylic acid, Omeprazol, methotrexate, meloxicam, Adalimumab for arthritis

* Genetic testing was not possible due to unavailability of DNA, included due to similarity of clinical phenotype.

Table S2. Lymphocyte subset characterization in CHAPLE patient peripheral blood.

Clinical evaluation of patient peripheral blood lymphocyte subsets using flow cytometry gating. Bold indicates values outside of the normal range.

Table S2. Lymphocyte subset characterization in CHAPLE patient peripheral blood.

Patient ID	P 1.1	P 2.1	P 3.1	P4.1	P4.2	P4.3	P 5.1	P 5.2	P 6.1	P 7.1	P 8.1
Lymphocyte Subsets (% of lymphocytes)											
$CD3^+$	**86%** (55-78)	**87%** (55-83)	78% (55-78)	74% (43-76)	67% (55-83)	76% (55-83)	56% (55-78)	**80%** (55-78)	75% (52-78)	**78%** (43-76)	72 (55-77)
$CD3^+CD4^+$	44% (27-53)	47% (28-57)	28% (27-53)	47% (23-48)	37% (28-57)	38% (28-57)	27% (27-53)	44% (27-53)	**49%** (25-48)	37% (23-48)	**56%** (29.3-52.9)
$CD3^+CD8^+$	**38%** (19-34)	32% (10-39)	**39%** (19-34)	25% (14-33)	26% (10-39)	38% (10-39)	24% (19-34)	21% (19-34)	28% (9-35)	**37%** (14-33)	15% (13.5–22)
$CD19^+$	**1.5% (10-31)**	6% (6-19)	24% (10-31)	18% (14-44)	14% (6-19)	8% (6-19)	29% (10-31)	**8%** (10-31)	**6%** (8-24)	14% (14-44)	**19%** (7.8–15.1)
$CD3^-$ $CD16^+/CD56^+$	12% (4-26)	**3%** (7-31)	12% (4-26)	6% (4-23)	15% (7-31)	8% (7-31)	11% (4-26)	7% (4-26)	**1%** (6-27)	**3%** (4-23)	8% (7-26)

Table S3. Summary of homozygous autosomal recessive mutations in patients who underwent WES.

Homozygous mutations found in exome-sequenced patients matching an autosomal recessive pattern of inheritance. We further filtered out non-coding, common, and synonymous coding mutations leaving only rare (<1% in reference databases), splice site, insertion/deletion, nonsense, and non-synonymous missense mutations as potential candidates. For Family 5, variants highlighted in grey are only present in Patient 5.1.

Table S3. Summary of homozygous autosomal recessive mutations in patients who underwent WES.

Patient	Mutation Type	Gene	Chromosome	Start	Reference	Genomic Variant in Patient	Protein Variant in Patient
1.1	Missense	*RASAL2*	1	178063755	C	A	Ala43Asp
1.1	Missense	*FAM163A*	1	179783085	G	C	Gly89Arg
1.1	Missense	*RGSL1*	1	182499493	A	C	Lys747Thr
1.1	Missense	*DYRK3*	1	206811072	A	G	Asn52Ser
1.1	Deletion	*CD55*	1	207495774	GAA	G	Frameshift, Ter16
1.1	Insertion	*CD55*	1	207495776	AA	CCTT	Frameshift, Ter17
1.1	Essential Splice Site	*CR2/ CD21*	1	207647585	G	C	N/A
2.1	Deletion	*CD55*	1	207495734	TG	T	Frameshift, Ter24
2.1	Missense	*CEP290*	12	88480233	G	C	Asp1413His
3.1	Deletion	*CD55*	1	207495734	TG	T	Frameshift, Ter24
3.1	Missense	*RBM6*	3	50103737	G	C	Glu393Asp
3.1	Missense	*C3orf15*	3	119451267	C	G	Pro382Asp
3.1	Missense	*POLQ*	3	121179019	G	A	His2344Tyr
3.1	Missense	*FBXO40*	3	121342057	C	G	Ala594Gly
3.1	In-frame Deletion	*GATA2*	3	128205102	CCAC	C	His113del
3.1	Missense	*AMOTL2*	3	134089834	G	A	Arg148Trp
3.1	Missense	*POSTN*	13	38143472	A	G	Phe742Ser
3.1	Missense	*CYSLTR2*	13	49281414	G	A	Ser154Asn
3.1	Missense	*CCDC70*	13	52439563	G	C	Val17Leu
5.1	Deletion	CD55	1	207495734	TG	T	Frameshift, Ter24
5.1	Missense	POLR3G	5	89802423	G	A	Glu173Lys
5.1	Missense	GPR98	5	90119297	G	A	Val5418Met
5.1	Missense	CD27	12	6560484	C	A	Pro237Thr
5.1	Missense	ATF7IP	12	14577193	A	G	His123Arg
5.1	Missense	MRPS27	5	71516795	G	C	Gln410Glu

Table S4. Predicted impact scores for identified CD55 Variants.

Mutation and impact score calculated from either the SIFT, Polyphen2 and CADD predictive algorithms based on a reference sequence from ENST00000367064, GRCh37. This scoring system was not applicable (N/A) to INDEL mutations.

Table S4. Predicted impact scores for identified CD55 Variants.

Mutation	Chromosome	Position	SIFT	Polyphen2	CADD
c.149_150delAAinsCCTT	1	207495774	N/A	N/A	N/A
c.109delG	1	207495734	N/A	N/A	N/A
c.800G>C	1	207504588	0 (deleterious)	0.99 (probably damaging)	23.1
c. 287-1G>A	1	207497903	N/A	N/A	23.9
c.367insA	1	207495992	N/A	N/A	N/A

Figure S1. Extended pedigrees and chromatograms.

Extended pedigrees and DNA sequence chromatograms, grouped according to disease alleles, for families 1 and 7 (Panel A); families 2, 3, and 5 (Panel B); family 4 (Panel C); and family 6 (Panel D), and family 8 (Panel E) respectively. Affected individuals homozygous for disease alleles indicated by solid symbols, heterozygous individuals indicated by half solid symbols, and individuals with an unknown genotype indicated open symbols which are red if affected. Triangle indicates miscarriage. The double line indicates consanguinity. Chromatograms display the specific nucleotide mutations in the CD55 gene sequence in patients (P) compared to the reference (WT) with amino acids shown above the nucleotide sequence, when applicable.

Figure S1. Extended pedigrees and chromatograms

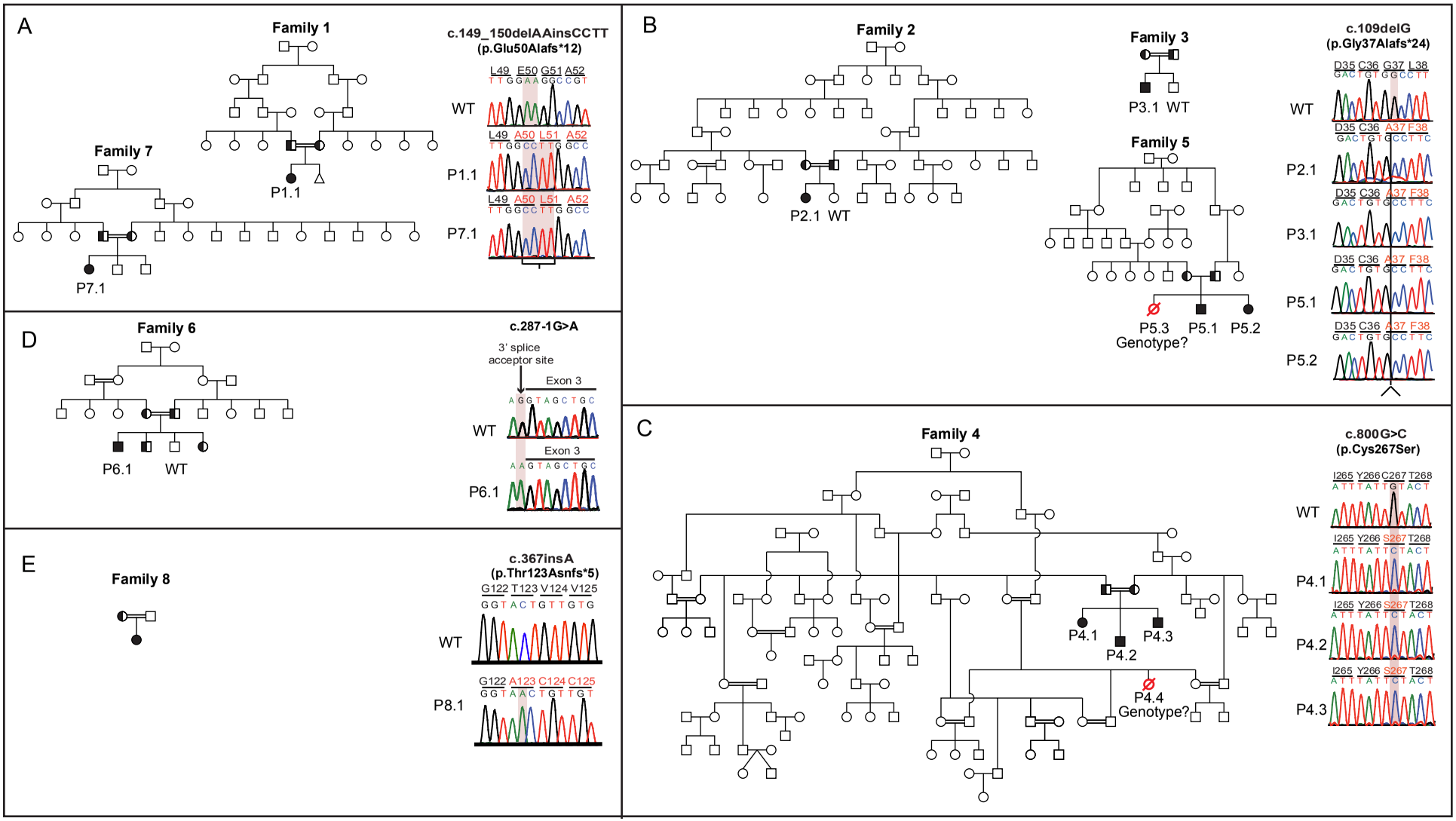

Figure S2. Albumin levels and weight/height curves of CD55 patients.

Panel A (left column) shows long term serum levels of immunoglobulin G (IgG, left Y axis) in relation to serum albumin (right Y axis) concentrations as a function of age in years for Patient 2.1, 3.1, and 4.1. Age-specific lower cutoff value for IgG is denoted by the red dotted curve, whereas the reference for albumin level is >3.5 g/dl (indicated by hatched line on right Y axis). Each arrow denotes an episode of pneumonia. Panel A (right column) shows short term serum albumin concentration in grams per deciliter (g/dl) from Patient 5.1 and 5.2 on a weekly basis and from Patient 6.1 over years (red). Abrupt rises reflect albumin transfusion, examples of which are indicated by a blue star in P6.1; black lines indicate the normal range. Green arrow indicates resection of lymphangiectatic segment in Patient 5.2, normalizing albumin levels. Panels B shows height (stature) and weight curves versus age in years for Patients 1.1, 2.1, 6.1, and 7.1 relative to the percent of the normal population (numbers at right) in each value.

Figure S2. Albumin levels and weight/height curves of CD55 patients.

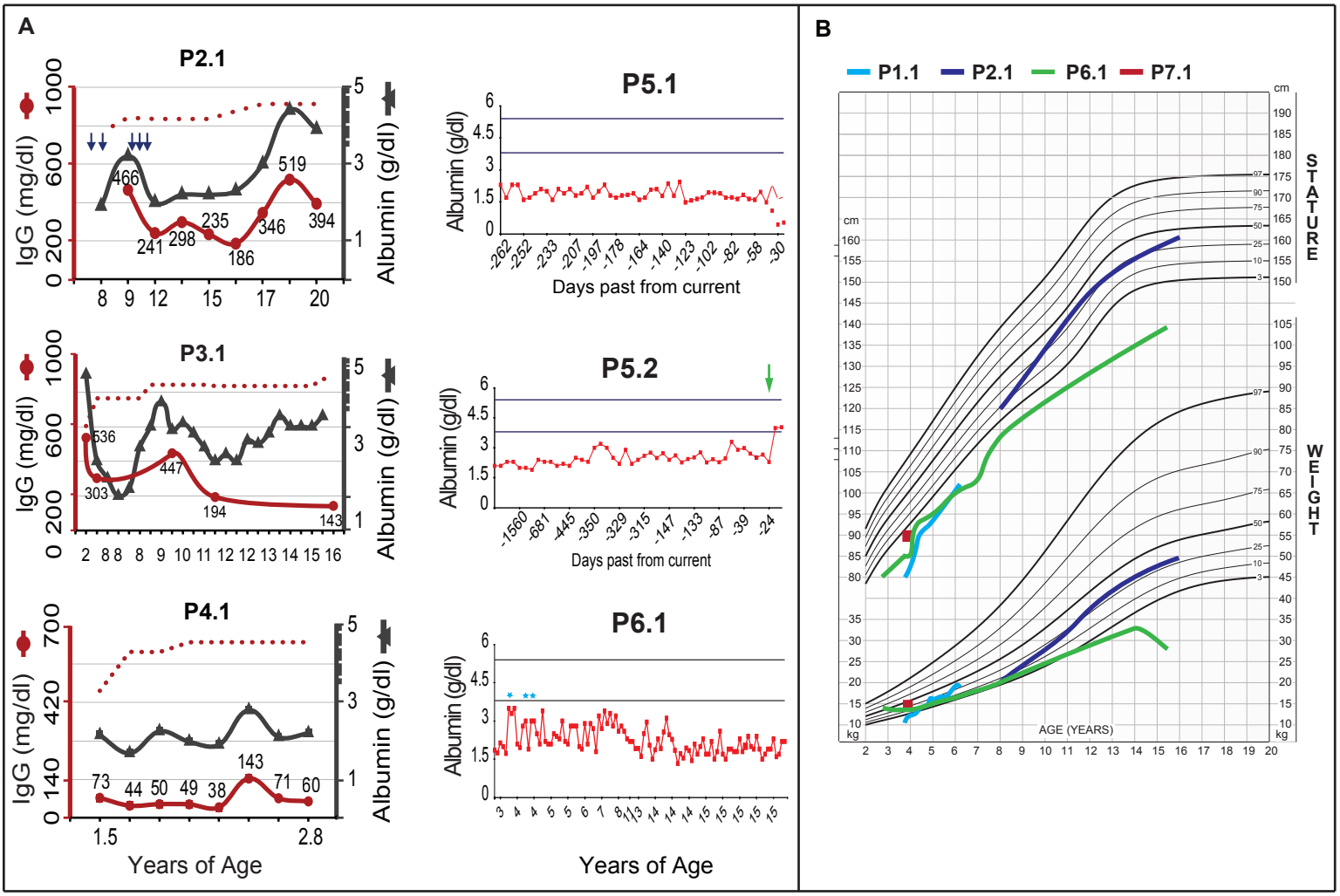

Figure S3. CD55 Deficiency is associated with pronounced primary intestinal lymphangiectasia and normal capillary endothelial barriers.

Panel A shows the hematoxylin and eosin stained histological section from the resection specimen from Patient 2.1 and immunohistochemical stains for PROX-1 and D2-40 (Podoplanin), markers of lymphatic endothelial nuclei and cell bodies, respectively, from the villi or submucosal (sm) regions with dilated lymphatic regions indicated by blue arrows. Panel B shows a representative transmission electron microscopy (TEM) image from a duodenal biopsy of Patient 6.1 showing edematous interstitium, dilated lymphatic vessel (blue arrows) and normal blood capillary (black arrow). Panel C shows TEM of endothelium in a duodenal biopsy and the red outlined section magnified 3X. Arrows show diaphragms spanning the fenestrae of the endothelial cells. Panel D shows an abdominal CT image from Patient 2.1 with intestinal obstruction with mucosal thickening of the distal ileal segments and luminal narrowing (the lead pipe sign, red arrow).

Figure S3. CD55 Deficiency is associated with pronounced primary intestinal lymphangiectasia and normal capillary endothelial barriers.

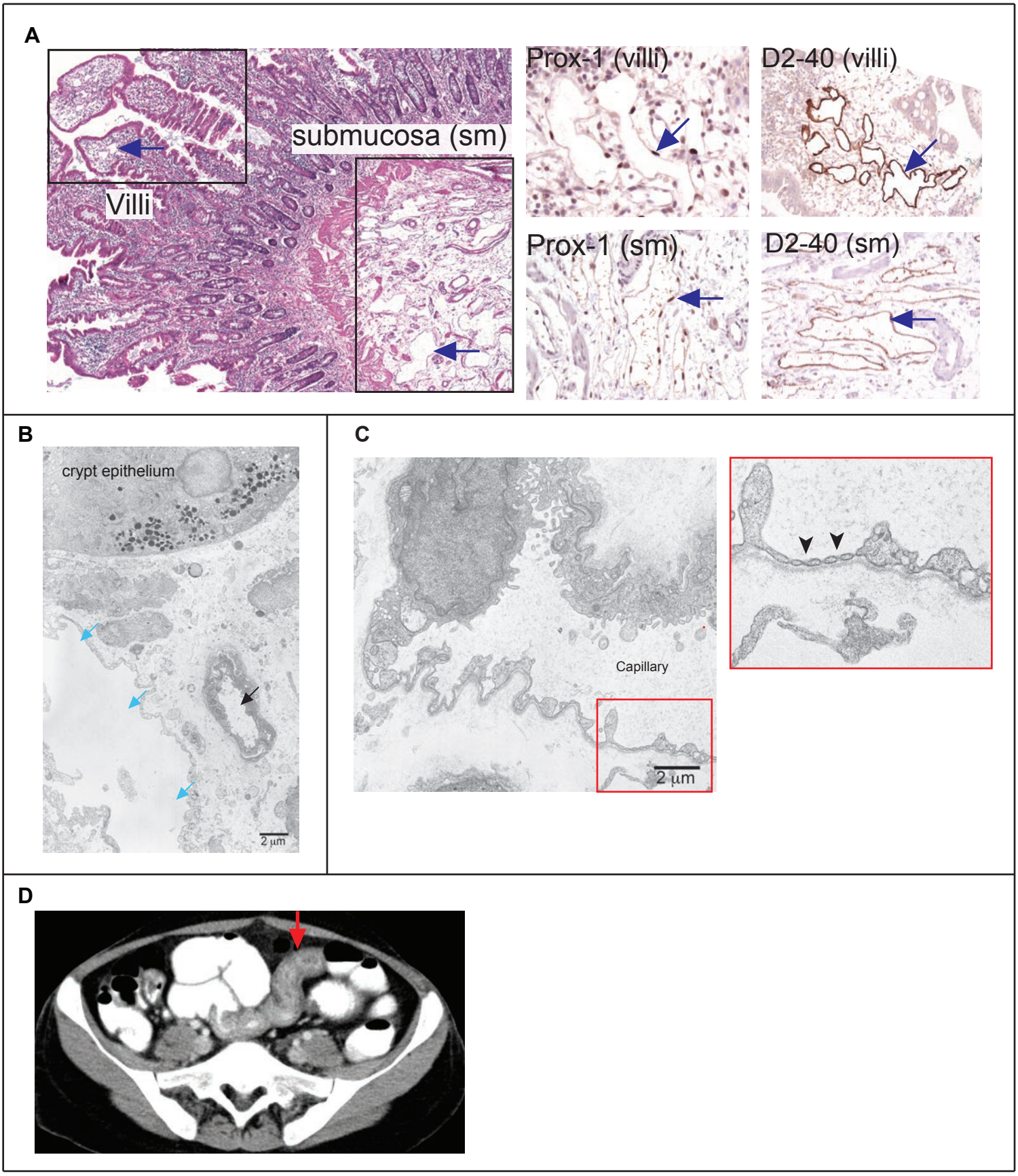

Figure S4. Inflammatory changes and bowel wall thickening in the intestinal tissue of CD55-deficient patients.

Panel A shows hematoxylin and eosin (H & E) sections of the colonic mucosa with focal lymphofollicular aggregates (*) in an endoscopic biopsy sample of Patient 2.1. Panel B shows H & E stained sections of a colonic biopsy specimen from Patient 3.1 at 200X (left) and 400X (right) magnification demonstrating reactive changes to the crypt epithelium (yellow arrow), lymphoid infiltrates (>>), and cryptitis (black arrow) and crypt abscess (green arrow). Panel C shows a radiological GI exam in Patient 6.1. Double arrows indicate diffuse target-water small bowel wall enhancement and single arrow indicates scattered area of dilation.

Figure S4. Inflammatory changes and bowel wall thickening in the intestinal tissue of CD55-deficient patients.

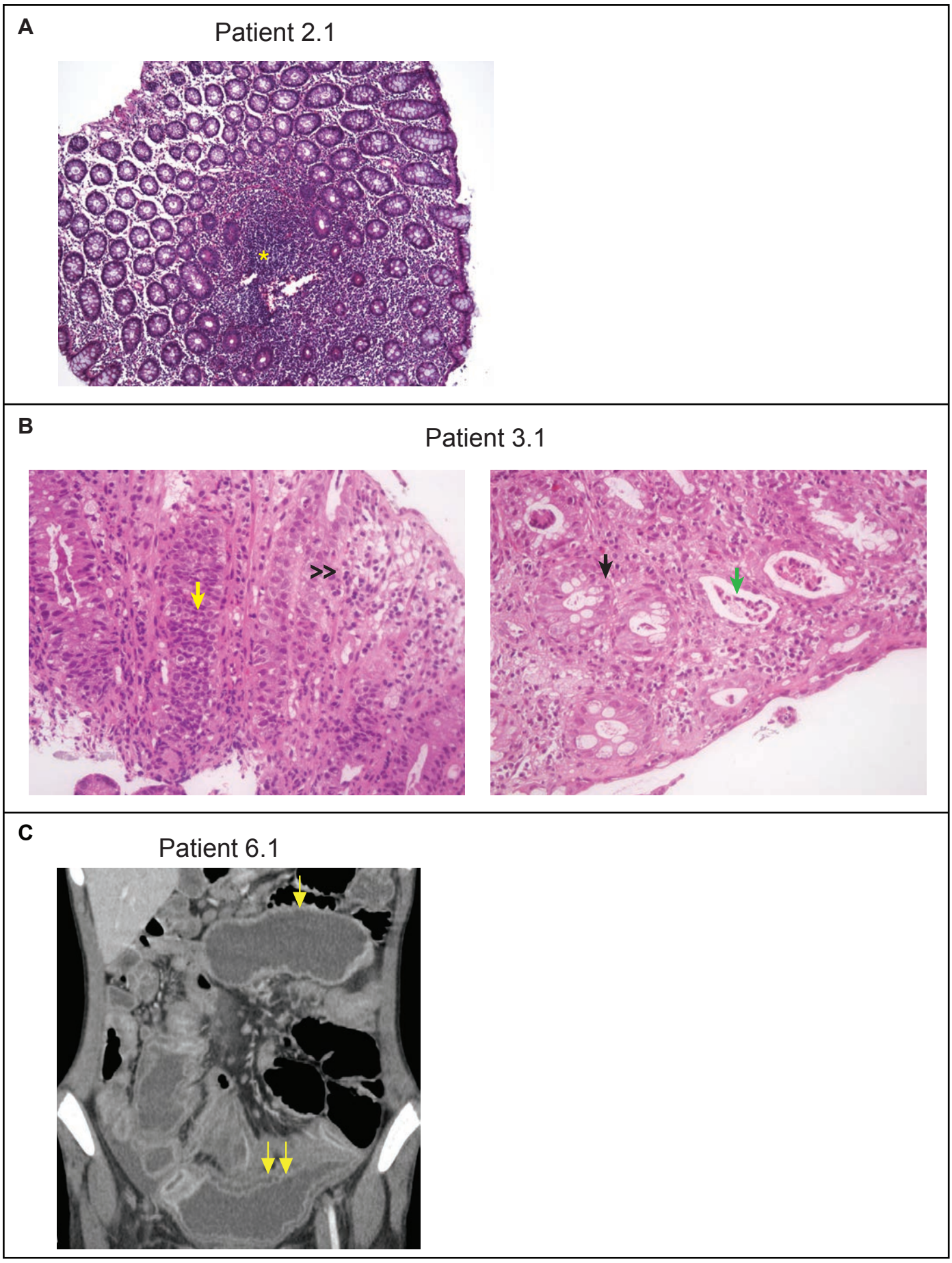

Figure S5. Assessment of B-cell subpopulations in CHAPLE patients by flow cytometry.

Panel A shows flow cytometry plots for CD21 (CR2) protein expression in gated patient (P) and control $CD19^+$ B cells. Panels B and C show flow cytometry plots of proportions of naïve B cells (IgD^+CD27^-) and class-switched memory B cells (IgD^-CD27^+) from P1.1 and P5.1. Panel D and E show quantification for multiple patients compared to age-matched healthy controls.

Figure S5. Assessment of B-cell subpopulations in CHAPLE patients by flow cytometry.

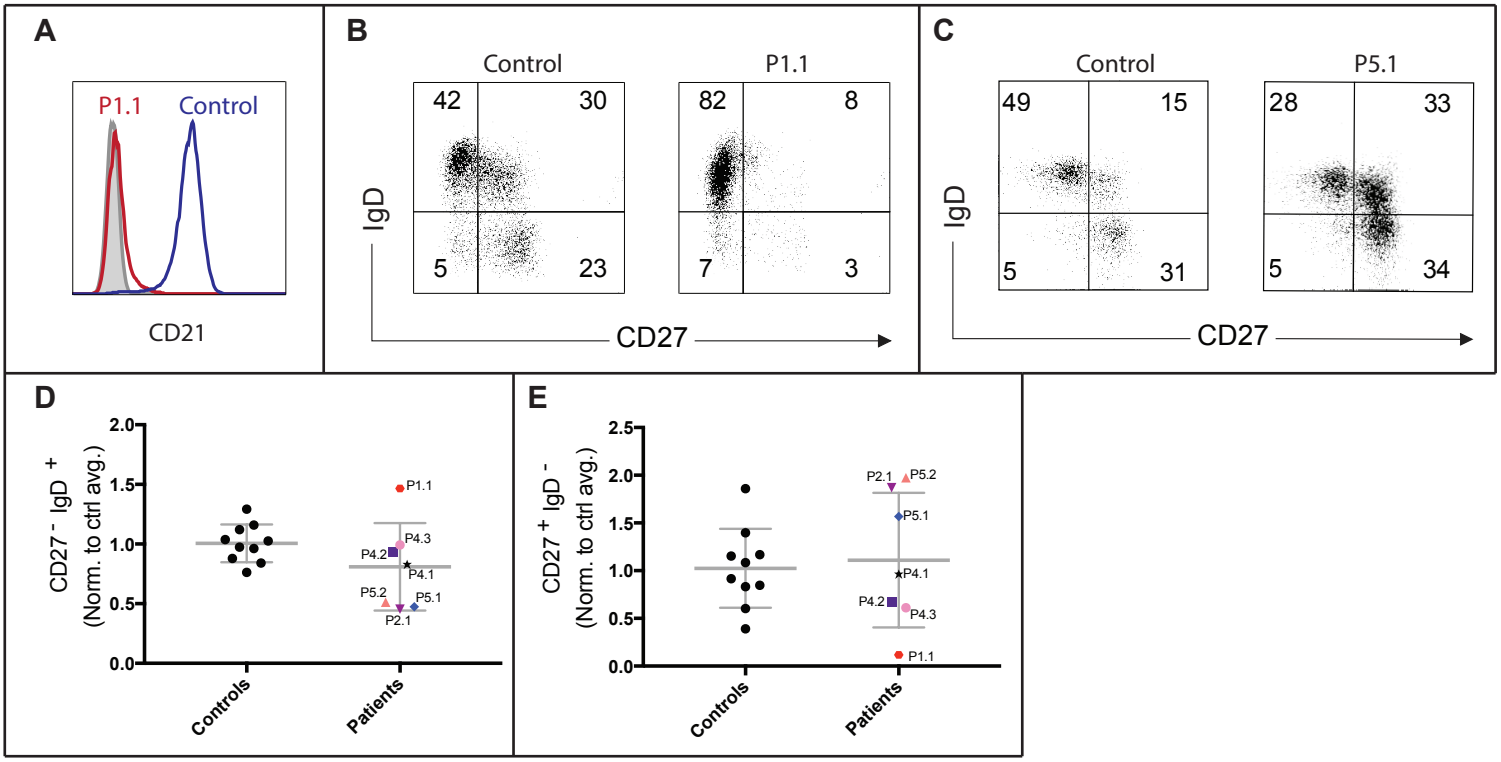

Figure S6. CD55 deficiency is associated with thrombotic events and erythrocyte/endothelium interactions and translocation to the interstitial space.

Panel A shows a multiplanar reformatted volume rendered (MPVR) axial CT from Patient 6.1 showing pulmonary embolus and lack of vascular flow in right pulmonary artery branches (yellow arrows, left) and an MPVR image from Patient 6.1 showing irregular peripheral arteriovenous malformations (blue ovals, right). Panel B shows two representative pictures of erythrocytes attaching to capillary endothelial walls (black arrows). Panel C shows transmural migration of erythrocytes (black arrows) and numerous erythrocytes in the interstitial space. Panel D shows an epithelium layer detaching from the basement membrane creating an abnormal space (blue stars), and numerous erythrocytes in the sub-epithelial interstitium (red E). For panels B, C, and D, the red letter E indicates erythrocytes outside of a capillary while black letter E indicates erythrocytes within a capillary. Panel E shows immunofluorescence staining of a healthy donor duodenal biopsy. In the duodenal submucosa (SM) CD55 is expressed on endothelial cells in the basal (white arrows), but not upper submucosa (yellow arrows). In duodenal villi CD55 was expressed along the brush border of the columnar epithelium (white arrows) with low/medium expression on capillary endothelial cells (yellow arrow) and high expression on lymphocytes (blue arrows) within the lamina propria.

Figure S6. CD55 deficiency is associated with thrombotic events and erythrocyte/endothelium interactions and translocation to the interstitial space.

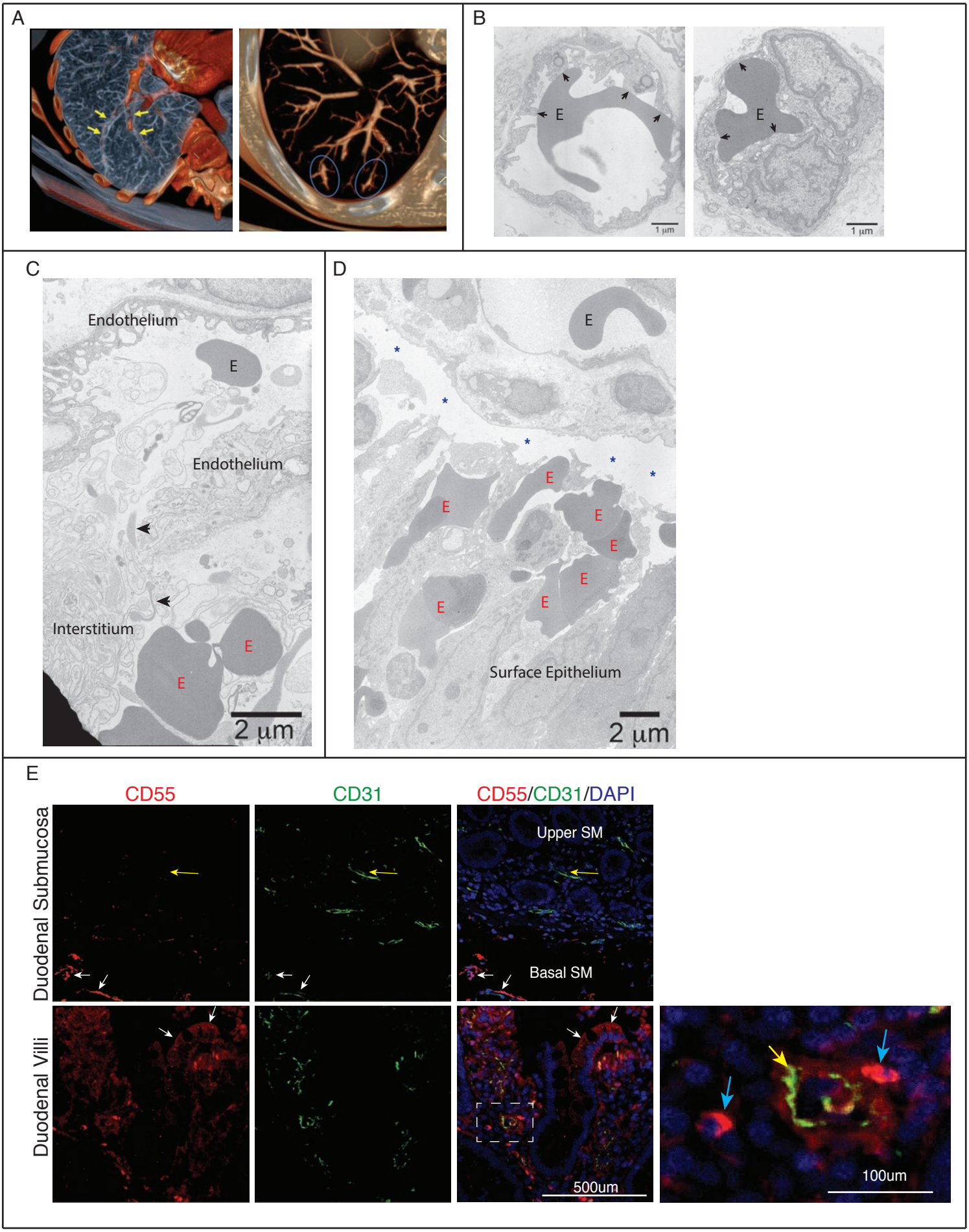

Figure S7. Patient genetic variants in CD55 lead to loss of mRNA and protein expression.

Panel A shows the life cycle of the alternative pathway C3 convertase formation and regulation by the two mechanisms of 1) reversible decay-acceleration by CD55, FH, and CR1 and 2) the irreversible C3b cleavage mediated by Factor I and the cofactors CD46 and Factor H. As indicated, the antibody used to detect surface bound complement in this study binds an epitope in the C3d region of C3, and will detect all forms except C3a and C3c. Panel B shows the CD55 gene structure with indicated mutations confirmed during this study in black and mutations previously observed in Inab individuals [7-11]. Text color indicates Inab mutations with (red) and without (blue) a GI phenotype, respectively. Panel C shows qRT-PCR measurement of *CD55* mRNA in cycling CD4+ T-cell blasts from patients (P) or normal controls (NC). Panel D shows flow cytometry histograms of CD55 surface expression on CD4+ T lymphocytes for the patients compared to control. Gray histogram shows isotype control and the red histogram denotes experimental sample. Panel E shows the location of the amino acid substitution (Cys267Ser, position in green) in Family 4 within the ribbon diagram of the crystal structure of wild type CD55 protein. Panel F shows magnification of the affected disulfide bond (yellow) in SCR4 of wild type CD55.

Figure S7. Patient genetic variants in CD55 lead to loss of mRNA and protein expression.

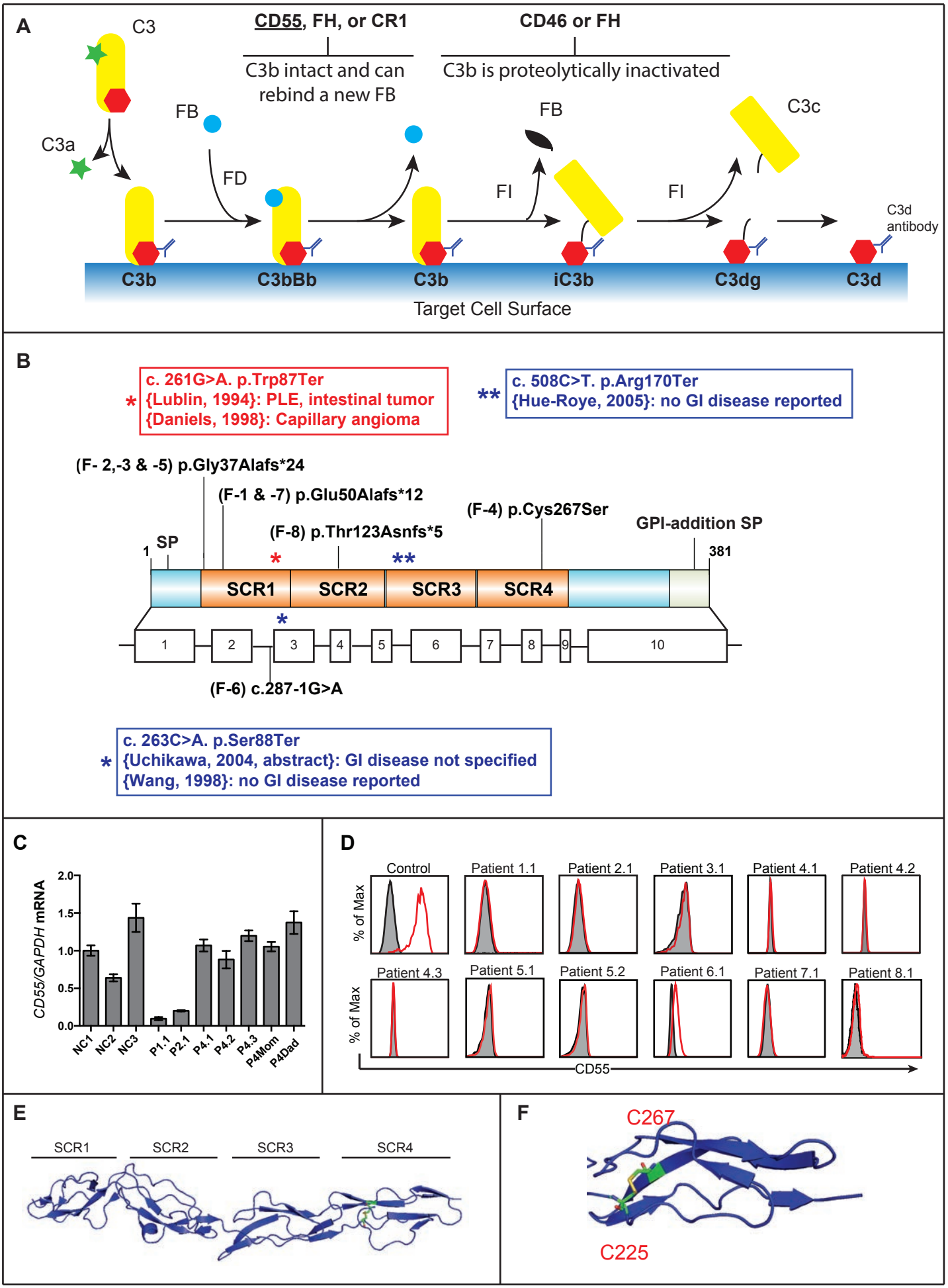

Figure S8. Changes in inflammatory cytokine production by CD55 deficient cells promote pro-thrombotic changes in endothelial cells.

Panels A, B, and C, respectively, show TNF, IL10, or IFNγ secretion in control and patient (P) T cells following restimulation with anti-CD3 for 48 hours. Cells were either left untreated or treated with a combination of C3aR and C5aR1 anaphylatoxin receptor inhibitors (ARi) at 10 μM. Each patient point represents the average (avg) of at least three independent experiments. Panel D shows TNF production in healthy donor cells stimulated for 48 hrs with 1 μM anti-CD3 alone (Stim) or with 10 μM of the indicated anaphylatoxin receptor inhibitor (aRi). Panel E shows flow cytometry plots of Thrombomodulin (CD141) and Tissue Factor (CD142) expression on HUVECs with either TNF (10 ng/mL), IFNγ (100 ng/mL), or both. Representative of 3 independent experiments. Panel F shows quantification as percent of control (cont) of CD55 expression on HUVECs with increasing doses of TNF. Statistics are performed on the average of at six independent experiments. Panel G shows quantification of CD55 expression on HUVECs treated with increasing doses of all trans retinoic acid (ATRA). Statistics are performed on the average of three independent experiments. Panel H shows Carboxyfluorescein N-hydroxysuccinimidyl ester (CFSE) dilution in normal control (NC) or patient (P) 1.1 T cells stimulated with 10 ug/mL anti-CD3 and the indicated co-stimulatory molecules. The fraction of cells the have divided according to the indicated gate is shown. Representative of three independent experiments. Panel I shows IL-10 production in normal control (NC) and patient (P) T cells stimulated with anti-CD3 and stimulatory antibodies directed against the indicated costimulatory molecules. Error-bars are calculated from technical replicates and results are representative of three independent experiments. (not significant (n.s.), * $p<.05$, ** $p<.01$, *** $p<.001$).

Figure S8. Changes in inflammatory cytokine production by CD55 deficient cells promote pro-thrombotic changes in endothelial cells.

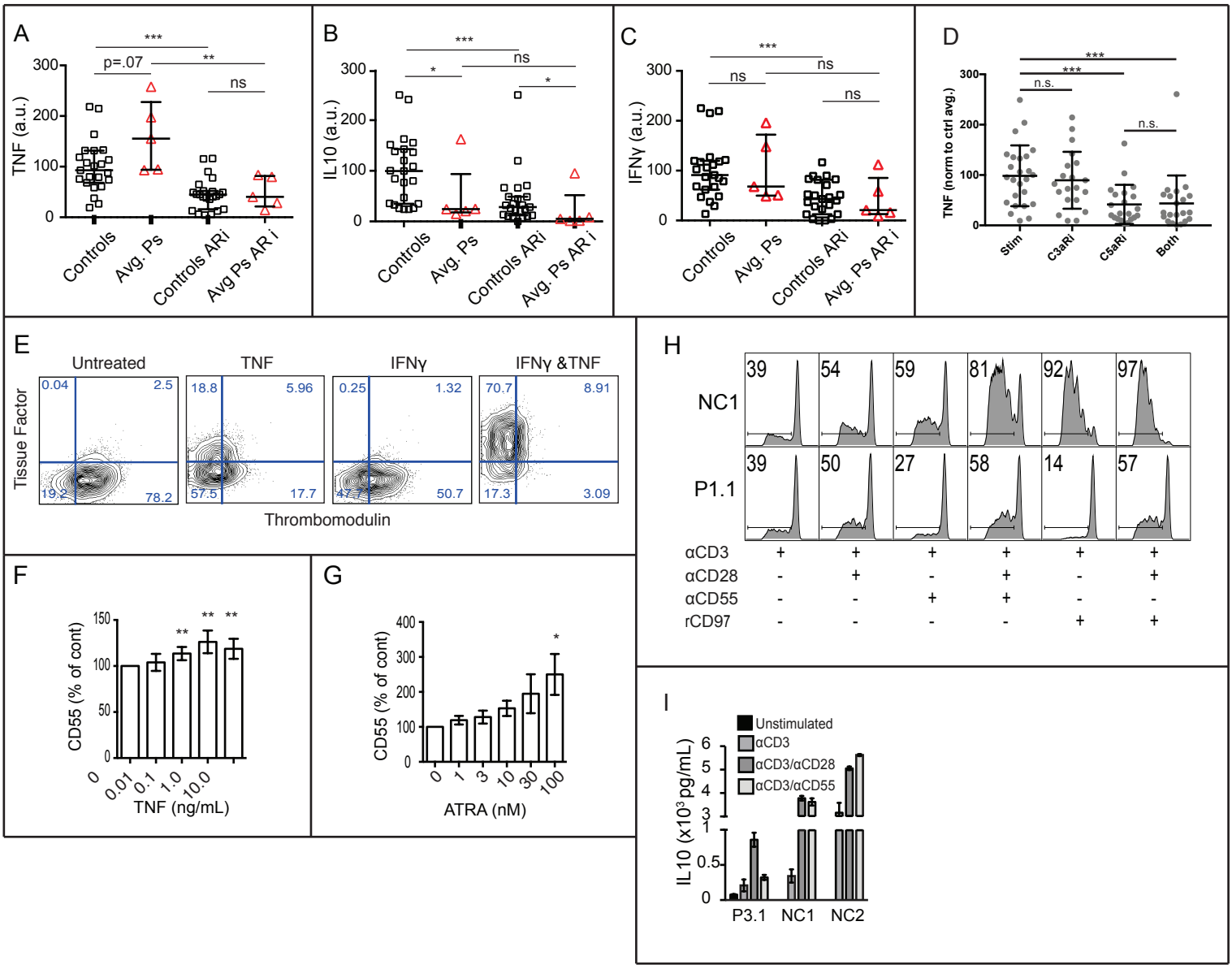

Figure S9. Model of the molecular pathogenesis leading to PLE in CHAPLE syndrome.

The proposed model shows how cellular pathology in the intestine leads to features of CHAPLE syndrome. Pro-inflammatory and pro-coagulant changes produce excessive complement effectors potentially during immune responses to the gut microbiome. This leads to endothelial and epithelial damage and lymph vessel distortion and compromised lymphatic flow causing lymphangiectasia, GI protein loss, and malabsorption of fat and micronutrients. This is associated with mucosal edema due to hypoproteinemia, pathological inflammation and lymphocyte infiltration due to cytokine changes, and intraluminal complement activation thus compromising intestinal epithelial barrier function. This, combined with hypercoagulability within blood vessels impairs normal circulatory dynamics, thus exacerbating PLE.

Figure S9. Model of the molecular pathogenesis leading to PLE in CHAPLE syndrome.

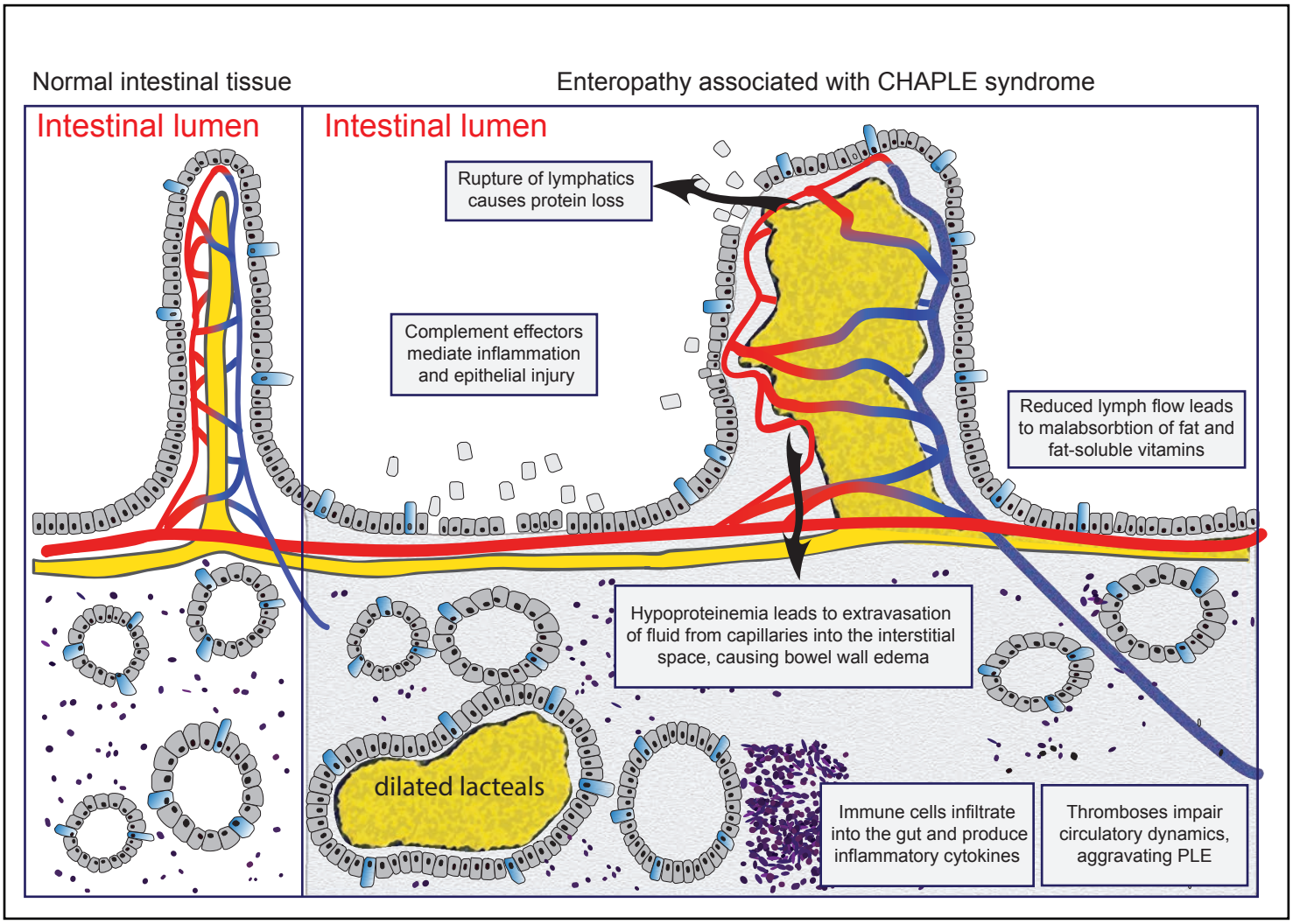

REFERENCES

1. Lucas CL, Kuehn HS, Zhao F, et al. Dominant-activating germline mutations in the gene encoding the PI(3)K catalytic subunit p110delta result in T cell senescence and human immunodeficiency. Nature immunology 2014;15:88-97.
2. Lucas CL, Zhang Y, Venida A, et al. Heterozygous splice mutation in PIK3R1 causes human immunodeficiency with lymphoproliferation due to dominant activation of PI3K. J Exp Med 2014;211:2537-47.
3. Leone DA, Kozakowski N, Kornauth C, et al. The Phenotypic Characterization of the Human Renal Mononuclear Phagocytes Reveal a Co-Ordinated Response to Injury. PLoS One 2016;11:e0151674.
4. Hubert V, Peschel A, Langer B, Groger M, Rees A, Kain R. LAMP-2 is required for incorporating syntaxin-17 into autophagosomes and for their fusion with lysosomes. Biol Open 2016;5:1516-29.
5. Ran FA, Hsu PD, Wright J, Agarwala V, Scott DA, Zhang F. Genome engineering using the CRISPR-Cas9 system. Nature protocols 2013;8:2281-308.
6. Sanjana NE, Shalem O, Zhang F. Improved vectors and genome-wide libraries for CRISPR screening. Nat Methods 2014;11:783-4.
7. Daniels GL, Green CA, Mallinson G, et al. Decay-accelerating factor (CD55) deficiency phenotypes in Japanese. Transfus Med 1998;8:141-7.
8. Lublin DM, Mallinson G, Poole J, et al. Molecular basis of reduced or absent expression of decay-accelerating factor in Cromer blood group phenotypes. Blood 1994;84:1276-82.
9. Wang L, Uchikawa M, Tsuneyama H, Tokunaga K, Tadokoro K, Juji T. Molecular cloning and characterization of decay-accelerating factor deficiency in Cromer blood group Inab phenotype. Blood 1998;91:680-4.
10. Hue-Roye K, Powell VI, Patel G, et al. Novel molecular basis of an Inab phenotype. Immunohematology 2005;21:53-5.
11. Yazer MH, Judd WJ, Davenport RD, et al. Case report and literature review: transient Inab phenotype and an agglutinating anti-IFC in a patient with a gastrointestinal problem. Transfusion 2006;46:1537-42.